Biomechanical Response of Male Post-Mortem Human Subjects to Vertical Drop Tower Testing and Application for Finite Element Model Validation

Timothy DeWitt, Alex Bendig, Angelo Marcallini, Yun-Seok Kang, John H. Bolte IV

Abstract The current study evaluates kinematic response of three male post-mortem human subjects (PMHS) during 15 G peak vertical drop tower testing. PMHS were instrumented using pressure sensors in the intervertebral discs from L2-S1 and 6DX blocks were rigidly coupled at T1, T4, T12, L3, and S1 to record spinal kinematics. Subjects were positioned in a rigid seat with a 90-degree seat pan-to-seatback angle and restrained using a pilot torso harness secured at the shoulders and a lap belt. Forces were estimated throughout the lumbar spine using intervertebral disc cross-section measurements and recorded pressure data. Peak z-axis acceleration for T1 through T12 ranged from -11.9 G to -24.3 G, whereas peak acceleration in the L3 and S1 regions ranged from -18.8 G to -40.9 G. Average calculated force in the lumbar spine ranged between 5.8 kN and 9.8 kN, with the highest values for PMHS1 and PMHS3 seen at L5-S1 and at L3-L4 for PMHS2. Post-test dissection revealed a minor compression burst fracture at T10 for PMHS1 and a left transverse process fracture at L2 for PMHS2, whereas no injuries were observed in PMHS3. Data will be used for future Finite Element Human Body Model validation efforts.

Keywords Lumbar spine response, thoracic spine response, vertical loading, vertical drop tower, PMHS.

I. INTRODUCTION

Ejection from high-performance aircraft, such as fighter jets, can expose individuals to vertical accelerations as high as 18 times the force of gravity [1]. Previous studies to evaluate the frequency of these events have shown ejection rates as high as 10–50 per year within the United States Air Force (USAF) alone [2] and spinal injury rates for legacy ejection systems as high as 30% to 61.6% [3-5]. In addition to concern for the well-being of the individuals both immediately following the event and long-term, this poses a great financial risk to government organizations, should the pilot be unable to return to service. On average, the cost per pilot for adequate training of aircraft operation can range from $5.6 million to $10.9 million [6]. Therefore, it is important to ensure the adequate safety of these ejection systems during operation so that pilots can escape unharmed and return to service.

Compressive spine injuries are of concern to the USAF and partner nations. They are evaluated as part of the qualification process for the ejection systems to ensure appropriate occupant safety and minimal probability of injury. Currently, the means for evaluating spinal injury probability is through physical experimentation with Anthropomorphic Test Devices (ATDs) and the determination of the Dynamic Response Index (DRI) [7]. The DRI was developed in the 1970s as a method of predicting the probability of injury based on spinal compression. However, the method relies on a second-order differential equation that relates the experimentally recorded accelerations from the ejection seat itself, and not any physical measure from the reaction of the occupant [8]. The model also assumes only a single axis of motion and utilizes assumptions for parameters such as vertebral column stiffness and body mass from a 50th percentile male, but it does not account for variation in occupant size or sex. These, along with other assumptions for valid use, such as specific restraint systems and occupant spine alignment with the acceleration vector, have led to the desire for alternative, updated methods for providing a more robust and accurate solution for injury prediction by using occupant response kinematics in lieu of seat or fixture accelerations.

Finite Element (FE) Human Body Models (HBMs) are actively being developed and used by the automotive industry as tools for safety system evaluation. Two primary contributors to these model development efforts have been Toyota Motor Corporation and the Global Human Body Models Consortium (GHBMC), which have developed the Total Human Model for Safety (THUMS) AM50 v6.1 and the GHMBC M50-0 v6.0 models, respectively. Each model provides a detailed representation of a 50th percentile male occupant and has been

T. DeWitt (e-mail: dewitt.167@buckeyemail.osu.edu; tel: +19376721079) is a PhD student and A. Bendig, A. Marcallini, Y-S. Kang and J. Bolte are staff and faculty at The Ohio State University, Columbus, OH.

validated both at the component level as well as using full-body sled test data for several automotive use cases in frontal, lateral, and rear impacts [9-10]. The validation of these models to the vertical loading environment though has been limited and focused primarily on the use of functional spinal units (FSUs). A small number of studies have been done to evaluate full-body FE HBM response using PMHS. However, those applications focused on use in underbody blast scenarios and lower extremity response [11-12]. The purpose of this study is to develop 50th percentile male PMHS responses sufficient for use in FE HBM model validation during vertical loading similar to that seen during aircraft ejection.

II. METHODS

Subject Procurement and Instrumentation

Approximate 50th percentile male PMHS (N=3) were obtained through the Ohio State Body Donation Program. All subjects were screened using Dual-Energy X-ray Absorptiometry (DEXA) to ensure areal bone mineral density (aBMD) scores were above an osteopenic range in the lumbar spine (lumbar T-score>-1.0). Other initial subject acceptance criteria included age (24–60 years), weight (60–95 kg), stature (160–190 cm), and body mass index (<30). After initial screening using DEXA, CT scans were performed for all subjects to check for unacceptable spine abnormalities in both the lumbar and thoracic spine regions. Detailed anthropometric measurements were taken for all subjects to characterize dimensions thought to play a role in subject response. Overall, subject weight, stature, and torso size were deemed relevant as potential contributors to expected response data, and a summary of these measurements is included in Table I.

TABLE I
ANTHROPOMETRIC MEASUREMENTS

	Weight (kg)	Stature (cm)	Sitting Height (cm)	Chest Circumference (cm)	Waist Circumference (cm)	aBMD T-score (L1-L4)
PMHS1	80.5	173.5	84.9	104.9	96.6	-0.6
PMHS2	76.8	183.0	89.3	96.5	103.5	0.7
PMHS3	94.8	182.5	92.7	101.2	105.3	0.2

Subject spinal kinematics were recorded using 6 degree-of-freedom (6DOF) motion blocks (6DX, DTS, Seal Beach, CA, USA) at T1, T4, T12, L3, and S1. At each level, a custom mount was rigidly fixed to the body to allow for mounting of the instrumentation. Pressure sensors were inserted into the center of the intervertebral discs at L2-L3, L3-L4, L4-L5, and L5-S1 to record internal pressure during the loading event. To place these sensors, the CT images of the PMHS were used to determine the approximate A-P depth of the intervertebral discs (IVDs) of interest. A surgical needle (10 gage, North American Rescue LLC, Greer, SC, USA) was inserted halfway through the disc to create a sufficient passage before securing the sensor in place using adhesive. Exemplary 6DX motion block mount and pressure sensor are shown in Fig. 1.

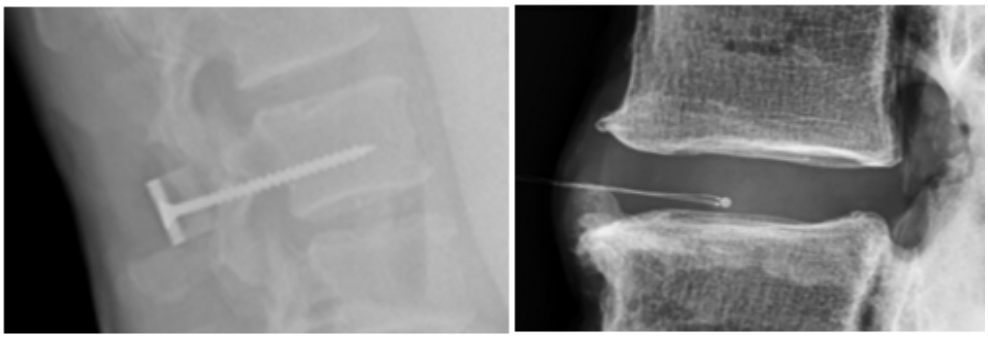

(a) (b)

Fig.1. (a) 6DX block mount and (b) pressure sensor placement.

After completing the instrumentation installation, a pre-test CT scan was performed to document instrumentation positions and orientations.

Test Facility and Fixture

The Vertical Deceleration Tower (VDT) at Wright-Patterson Air Force Base, Ohio, was used to generate the vertical pulse for the study. The VDT is composed of two vertical guide rails, approximately 15 m in length, and a carriage (Fig. 2). The occupant seating system is attached to the carriage and raised up the guide rails to the target drop height, which is calculated based on the desired peak deceleration. When released, the carriage free falls down the guide rails into a water brake system at the bottom, producing a decelerative pulse equal in magnitude and direction to the accelerative pulse the pilot would experience during ejection. For this study, the seating system used was a custom-designed rigid seat, with a 90° seat pan-to-seatback angle.

Fig. 2. VDT and experimental seat.

The seat also incorporates an adjustable headrest, footrest, and adjustable shoulder- and lap-belt anchor points. Accelerometers were placed on the VDT carriage to record the achieved vertical deceleration, and four six-axis load cells were placed underneath the seat pan to record the total reaction force on the seat imposed by the occupant. The subject was restrained using a standard issue pilot torso harness, attached to the seat at the shoulders, and a lap belt anchored to the floor of the VDT carriage. The belts of the shoulder and lap were instrumented using inline load cells to capture the belt tension on each of the restraints.

PMHS Positioning and Pre-test Procedures

PMHS were fitted with the pilot torso harness and secured by a trained USAF Air Crew Flight Equipment specialist. Once fit, the PMHS was sat in the seat with the mid-sagittal plane aligned to the center of the seat-back, and the headrest was adjusted to align with the center of the PMHS head. The footrest of the fixture was adjusted such that the femora and tibiae were positioned at a relative 90° angle and the femora aligned with the horizontal. The shoulder strap height attachment points were adjusted to align the shoulder belt routing as close to horizontal as possible. Both shoulder belts and lap belts were pretensioned to 89 ± 22 N. Finally, the PMHS head was suspended in an upright position with the Frankfort plane aligned to the horizontal using overhead supports attached to the seat, designed to fail at sub-impact levels. Once the final position was confirmed, in-position X-rays were taken to document the subject spine curvature using a digital X-ray device. Digitization of the final occupant position was performed using FARO (Edge FaroArm, Faro Arm Technologies, Lake Mary, FL, USA) to document three-dimensional (3D) coordinates of specified anatomical landmarks as well as relative locations of the seat and restraint system. A 3D scan of the setup was also taken using the FARO laser scanner. The final setup for PMHS1 is captured in Fig. 3. The carriage of the VDT was raised to a pre-determined drop height to achieve a deceleration pulse of 15 G peak and rise time of approximately 70 ms with a duration of approximately 130 ms.

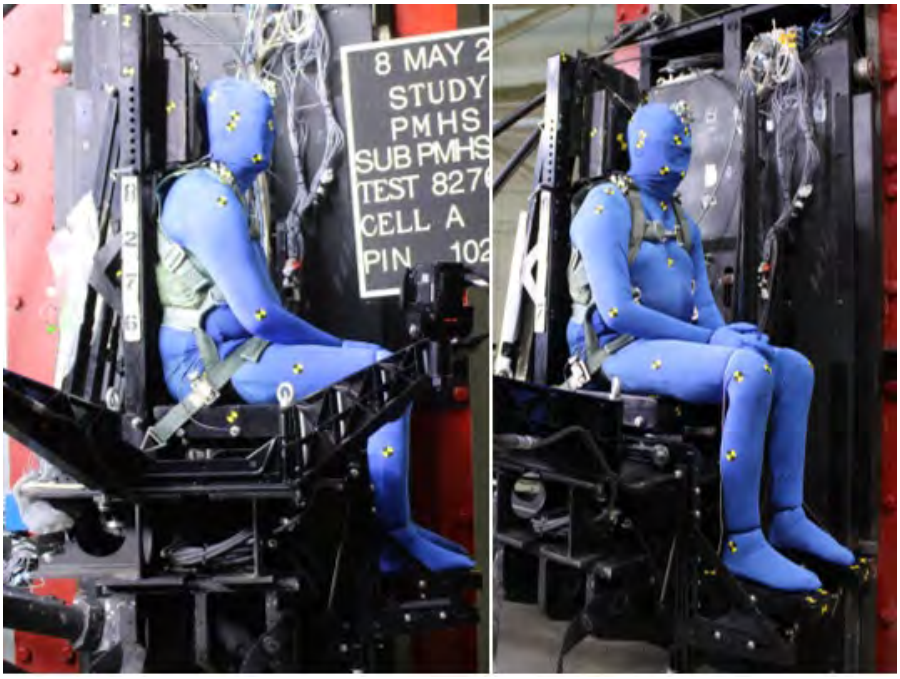

Fig. 3. PMHS final positioning (PMHS1).

Data Collection and Analysis

Two on-board data acquisition systems (SlicePro, DTS, Seal Beach, CA, USA) were housed on the VDT carriage and used to collect all data recorded during the test event. Both systems collected at a sample rate of 20,000 samples per second for all channels with 4,000 Hz anti-aliasing filter. Three high-speed cameras (two on-board and one off-board) were also used to record PMHS response at a sample rate of 1,000 frames per second. All load cells (seat and belt), 6DX, and linear accelerometers were zeroed with the PMHS seated in the final position before being raised up the VDT, and all recorded time-history data were processed in accordance with SAE J211 [13]. Spine 6DX motion block data were transformed to local anatomical coordinate systems described by Slykhouse *et al.* [14] using a custom MATLAB script.

Post-test Injury Analysis

Following each test, whole-body CT scans were used to document any injuries that may have occurred during the test. Post-test whole-body dissection was performed on each subject, with extra focus on the pelvis and spine. Any injuries found during dissection were documented by a certified Abbreviated Injury Scale (AIS) specialist.

III. RESULTS

PMHS Injury

Two out of the three PMHS (PMHS1 and PMHS2) subjected to testing experienced injury to the lumbar or thoracic spine region. PMHS1 sustained a minor compression fracture at T10 and a fracture at the coccyx (MAIS=2). PMHS2 sustained a fracture to the left transverse process at L2 (MAIS=1).

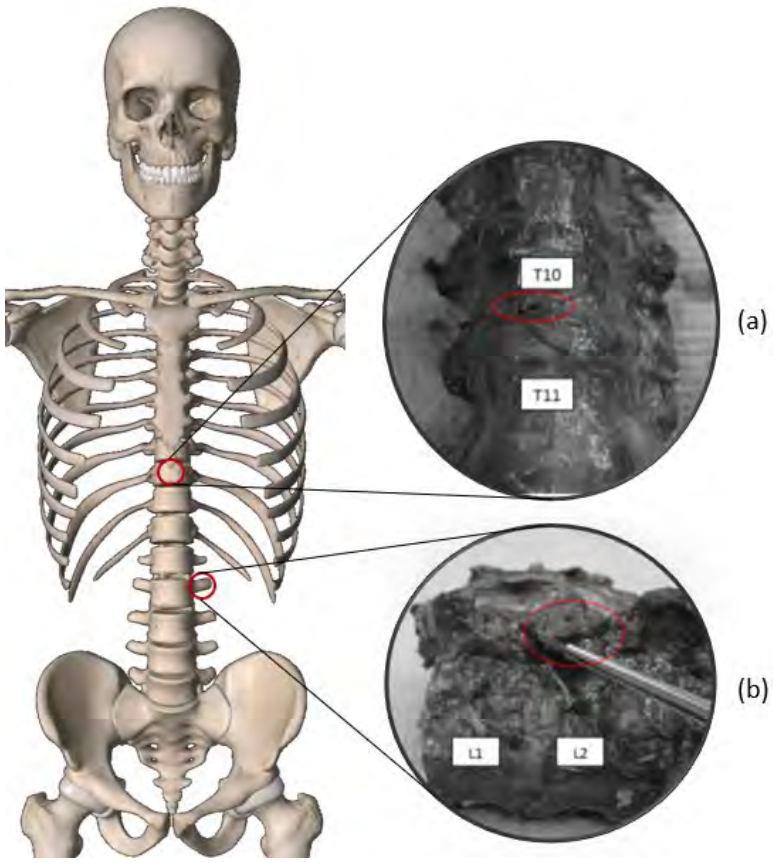

Fig. 4. (a) PMHS1 compression fracture and (b) PMHS2 transverse process fracture.

Fixture and Restraint Response

The desired 15 G peak acceleration was repeatably achieved between all tests (avg = -15.0 G, stdev = 0.1 G). The sum of the reaction forces within the seat pan was also consistent between PMHS1 and PMHS2 (avg = -15.7 kN, stdev = 0.3 kN). The highest seat pan reaction force was observed in PMHS3, which was to be expected, given PMHS3 was on the high end of the weight acceptance limit for the study. Time-history data for each of these can be found in Fig. A1 (see Appendix A).

Due to the routing of the torso harness and attachment points of the shoulder straps, shoulder strap belt loads may also play a critical role in the subject spine response. Left and right shoulder strap forces were averaged for each subject and are reported here (avg = 562.4 N, stdev = 51.3 N). Because of the compressive loading scenario, the contribution of the lap belt was found to be minimal, so those are not discussed. A digital T0 signal was recorded on the data acquisition system that was tied to a photodiode input and light source visible in the high-speed video footage. The signal undergoes a state change when the carriage crosses through the path of a laser housed on the fixture just before the start of the water break. This signal was used to zero all data. Timing between events was consistent, with high-speed video outcomes and between subjects showing, first, the recorded peak acceleration of the carriage (avg = 67.4 ms, stdev = 0.4 ms) followed by bottoming out of the subject in the seat and peak seat reaction loads (avg = 70.2 ms, stdev = 1.5 ms) and, finally, slight flexion forward of the subject and peak shoulder-belt force (avg = 95.7 ms, stdev = 0.7 ms). Peak response data are summarized in Table II and corresponding images for PMHS1 are shown in Fig. 5.

TABLE II
RESTRAINT AND FIXTURE RESPONSE

Subject	Carriage Z-acceleration (G)	Seat Force (kN)	Shoulder-belt Force (N)
PMHS1	-15.1	-15.9	584.9
PMHS2	-15.0	-15.6	503.6
PMHS3	-15.0	-18.9	598.6
Average	-15.0	-16.8	562.4
Standard Deviation	0.1	1.8	51.3

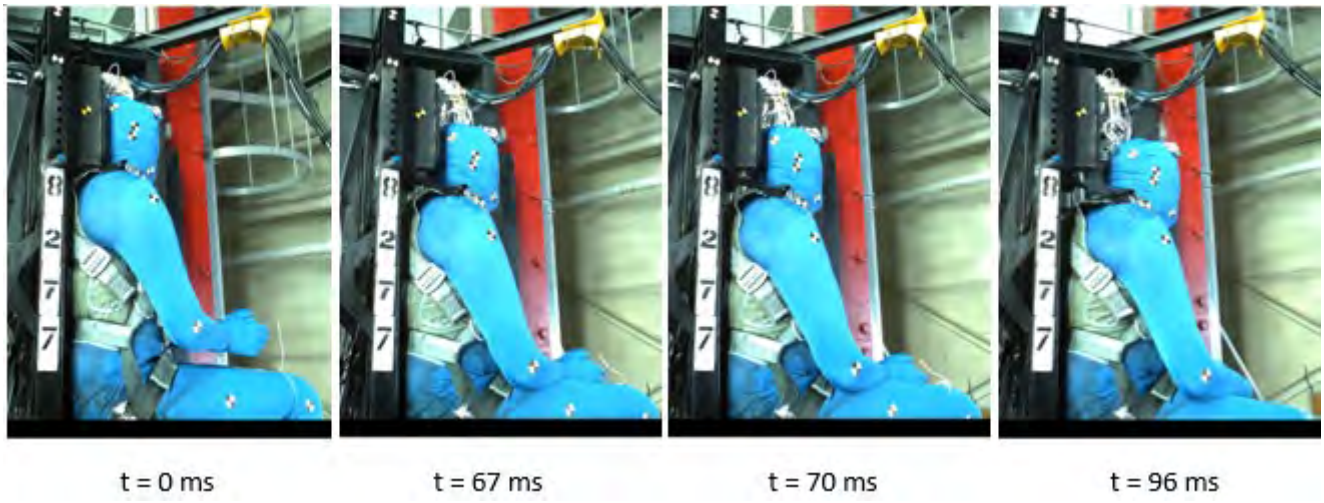

Fig. 5. High-speed video clips corresponding to peak fixture load event times (PMHS1).

PMHS Spine Kinematics

A summary of peak spine linear accelerations and y-axis angular velocity are shown in Table III and Table IV, respectively. PMHS1 experienced the highest resultant acceleration values at all recorded levels, with PMHS2 and PMHS3 generally trending more closely to one another. PMHS1 time-history data (Figs A2–A6) show sharp spikes in z-axis acceleration at all levels occurring consistently throughout recorded data at approximately 71 ms, which corresponds well to the peak reaction load time mentioned previously. Better agreement between PMHS peak resultant acceleration was seen at the superior instrumentation locations (T1, T4, and T12) compared to the more inferior locations (L3 and S1); however, there were no identified trends between levels. All PMHS show a consistent initial positive y-axis angular velocity (avg max = 289.3 deg/s, stdev = 4.4 deg/s) and positive x-acceleration at the S1 location, suggesting rearward tilt and forward movement of the pelvis, which is consistent with high-speed video. Instrumentation located at T4 showed opposite trends, with y-axis angular velocity (avg max = -711.1 deg/s, stdev = 115.0 deg/s) trending initially negative as well as negative x-acceleration, suggesting forward flexion of the torso combined with movement into the seatback. Those data were consistent with trends seen at T1; however, less consistent trends were seen at L3 and T12. Time-history data for S1 and T4 showing these trends are shown in Fig. 6.

TABLE III
PEAK SPINE LINEAR KINEMATICS SUMMARY

	Instrumentation	PMHS1	PMHS2	PMHS3	Average	Std Dev
T1	Peak resultant acceleration (G)	30.8	31.2	28.6	30.2	1.4
	Peak x-acceleration (G)	-29.8	-28.4	-28.5	-28.9	0.8
	Peak z-acceleration (G)	-18.7	-23.1	-11.9	-17.9	5.6
T4	Peak resultant acceleration (G)	33.5	23.8	27.9	28.4	4.9
	Peak x-acceleration (G)	-32.9	-23.5	-27.9	-28.1	4.7
	Peak z-acceleration (G)	-22.6	-15.8	-19.5	-19.3	3.4
T12	Peak resultant acceleration (G)	29.3	24.3	20.8	24.8	4.3
	Peak x-acceleration (G)	29.0	4.7	3.9	12.5	14.2
	Peak z-acceleration (G)	-24.3	-23.1	-20.6	-22.7	1.9
L3	Peak resultant acceleration (G)	41.9	27.1	27.3	32.1	8.5
	Peak x-acceleration (G)	11.3	17.3	6.4	11.7	5.5
	Peak z-acceleration (G)	-40.9	-19.9	-18.9	-26.6	12.4
S1	Peak resultant acceleration (G)	36.8	21.9	22.7	27.1	8.4
	Peak x-acceleration (G)	18.4	16.9	10.5	15.3	4.2
	Peak z-acceleration (G)	-31.8	-18.8	-20.3	-23.6	7.1

TABLE IV
PEAK SPINE ANGULAR KINEMATICS SUMMARY

	Instrumentation	PMHS1	PMHS2	PMHS3	Average	Std Dev
T1	y-axis angular velocity max (deg/s)	525.2	530.3	623.9	559.8	55.6
	y-axis angular velocity min (deg/s)	-579.4	-1132.6	-714.9	-809.0	288.3
T4	y-axis angular velocity max (deg/s)	367.7	308.4	347.0	341.0	30.1
	y-axis angular velocity min (deg/s)	-820.9	-591.4	-721.0	-711.1	115.0
T12	y-axis angular velocity max (deg/s)	394.1	102.2	81.5	192.6	174.8
	y-axis angular velocity min (deg/s)	-263.8	-215.1	-350.5	-276.5	68.6
L3	y-axis angular velocity max (deg/s)	204.2	112.0	203.1	173.1	52.9
	y-axis angular velocity min (deg/s)	-78.6	-69.5	-110.7	-86.3	21.7
S1	y-axis angular velocity max (deg/s)	287.9	285.8	294.2	289.3	4.4
	y-axis angular velocity min (deg/s)	-107.3	-87.9	-110.6	-101.9	12.2

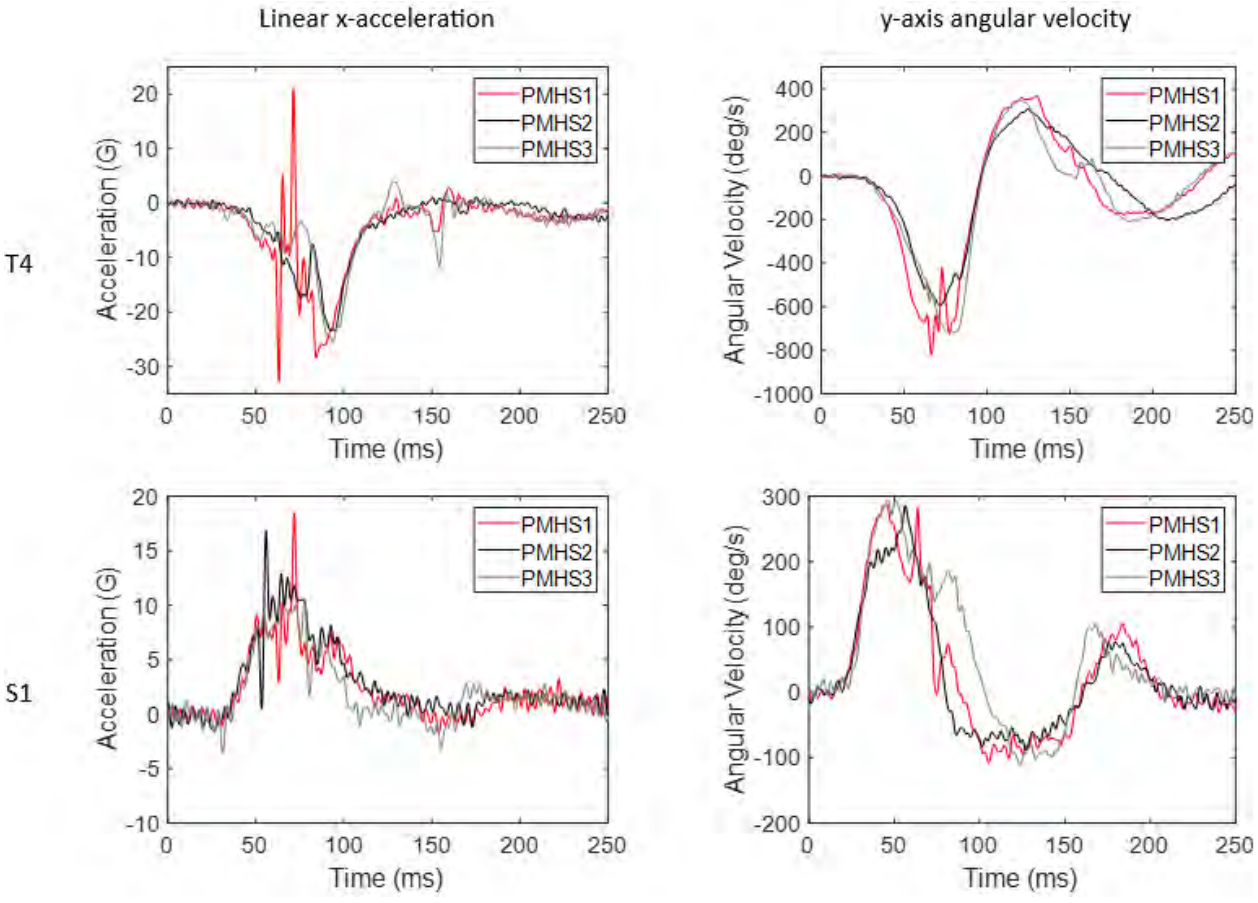

Fig. 6. Local x-acceleration and y-axis angular velocity for T4 and S1.

PMHS Lumbar Spine Force Estimates

Pressure data were successfully collected during each test. However, post-test data processing revealed channel malfunctions at L4-L5 and L3-L4 for PMHS3 and at L2-L3 for PMHS2. Pre-test CT scans were used to estimate the cross-sectional area of the discs where pressures were collected and subsequently used to calculate force at the desired levels. Area calculations for the disc assumed the disc to be a perfect ellipse. A summary of the disc measurements is presented in Table V, and the equation used for force calculation shown in Equation 1.

Table V

PMHS INTERVERTEBRAL DISC MEASUREMENTS AND CALCULATED AREAS

(AP = ANTERIOR-POSTERIOR AND LR = LEFT-RIGHT)

Vertebral Level	PMHS1			PMHS2			PMHS3		
	AP (cm)	LR (cm)	Area (cm^2)	AP (cm)	LR (cm)	Area (cm^2)	AP (cm)	LR (cm)	Area (cm^2)
L2-L3	3.9	5.5	16.9	4.9	6.4	24.5	4.7	6.0	21.9
L3-L4	4.4	5.9	20.4	4.7	6.6	24.6	4.6	6.1	21.9
L4-L5	4.1	6.0	19.3	4.9	7.1	26.9	4.5	6.4	22.4
L5-S1	3.7	5.2	15.2	4.5	6.8	24.0	4.2	6.2	20.7

$$F = P_{disc} * A_{disc} \quad (1)$$

Where F is the intervertebral disc force, P_{disc} is the recorded intervertebral disc pressure, and A_{disc} is the calculated disc area using Equation 2:

$$A_{disc} = \pi * \left(\frac{AP_{disc}}{2}\right) * \left(\frac{LR_{disc}}{2}\right) \quad (2)$$

The average calculated force for each PMHS ranged from 5.8 kN to 9.8 kN, which is lower when compared to the recorded sum of the reaction forces in the seat pan (15.6 kN to 18.9 kN) however, seems reasonable given the expected damping from the soft tissue in the body. Calculated force at L5-S1 showed good agreement between subjects (avg = 7.2 kN, stdev = 0.8 kN) and was the only level in which pressure was successfully collected in all three subjects. At the remaining levels, instrumentation difficulties resulted in one pressure sensor being lost in one of the PMHS during testing and therefore forces were not calculated. The greatest variability in calculated force was seen at L3-L4 (PMHS1 = 6.3 kN, PMHS2 = 9.8 kN). Peak values for each PMHS at individual levels are shown in Fig. 7.

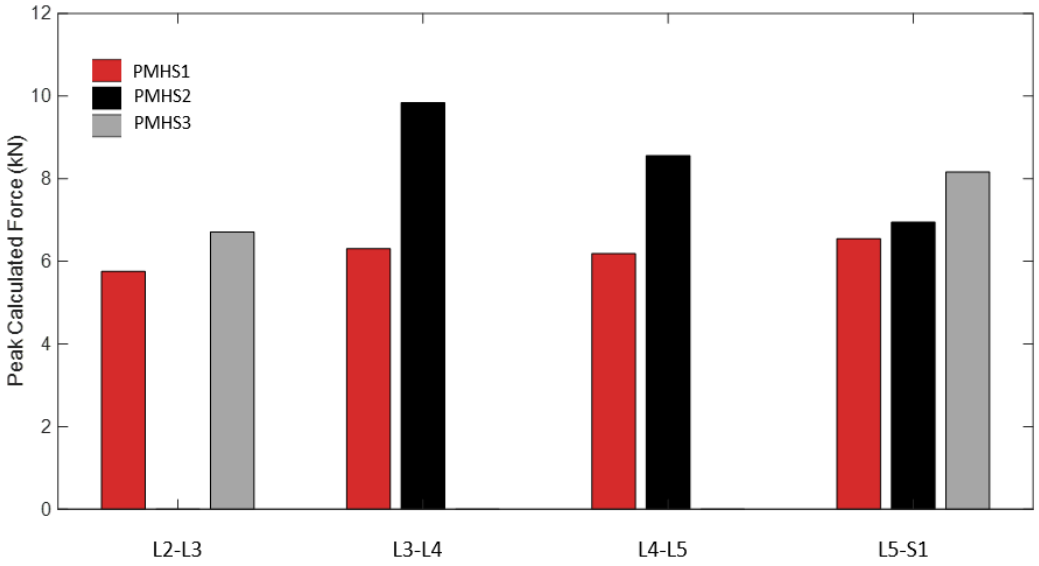

Fig. 7. Peak calculated forces in lumbar spine.

IV. DISCUSSION

PMHS Injury

This study aimed to generate male PMHS response data exposed to 15 G peak vertical acceleration, specific to the lumbar and thoracic spine. Both PMHS1 and PMHS2 sustained injuries to the spine; however, only PMHS1 sustained MAIS=2 injuries. PMHS1 also consistently reported the highest resultant acceleration among the three PMHS tested at all levels. Instrumentation was not present at the vertebral level of fracture (T10), making identification of exact fracture timing difficult. Investigation into the rate change of calculated force identified sharp increases throughout the intervertebral disc levels of L2-L3, L3-L4, and L5-S1 at approximately 70 ms. An increase was also seen in L4-L5 around the same time. However, these data seemed noisier overall than the rest. The isolated spikes in rate could be indicative of when the injury occurred and are consistent with the previously mentioned peak seat reaction load and maximum point of compression for the subject. The earliest recorded spike occurred at L2-L3 (70.45 ms) followed by L3-L4 (70.65 ms) and L5-S1 (70.70 ms), which supports injury superior to the instrumentation location and propagation down the spine. These data, as well as a still image of the occupant kinematics at that moment, are shown in Fig. 8.

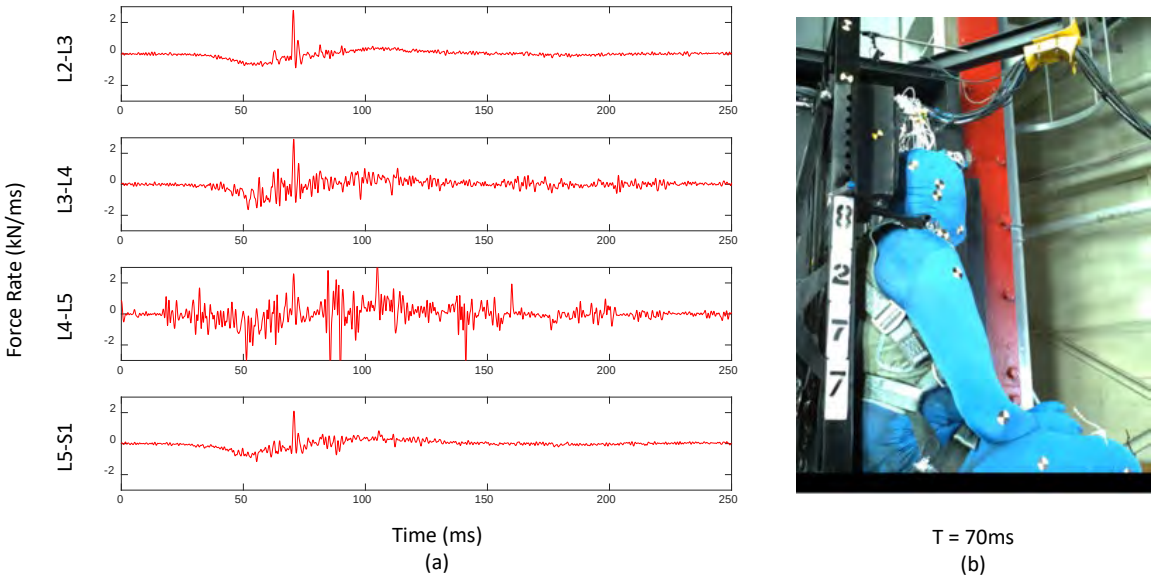

Fig. 8. (a) Calculated force rate for PMHS1 showing consistent spike through intervertebral levels and (b) corresponding high-speed video frame.

PMHS injuries observed during testing are consistent with operational injuries reported in literature. A systematic literature review of aircraft ejection data from 1971 to 2019 performed by Epstein *et al*. reported the most common spinal fracture location during ejection to be in the thoracic spine followed by the thoracolumbar junction and most commonly presenting as anterior wedge compression fractures [4]. Similar findings have been reported in a recent study by Sommer *et al*. who analyzed ejection injury data from the German Armed Forces from 1975 to 2021. Of the 103 cases identified, 66 vertebral fractures were observed of which, approximately 89% were in the thoracic or lumbar spine [5].

Fixture and Restraint Response

Fixture and restraint system response from the testing showed good repeatability in test conditions between subjects. Recorded reaction forces in the seat trended as expected with respect to subject weight and would most likely show increased repeatability if normalized based on subject mass. A similar trend was seen in the recorded shoulder-belt loads and could be considered for normalization as well at the conclusion of the study.

PMHS Spine Kinematics

Linear acceleration data collected for the vertebral bodies showed consistency between PMHS2 and PMHS3; however, PMHS1 consistently recorded the highest acceleration values. Spikes in acceleration data were correlated with the peak loading on the subject through seat reaction force data and peak force rates from the

lumbar vertebrae (Fig. 8). PMHS1 was also the only subject to experience a compression fracture during testing and, based on the consistency of the timing of spikes in recorded accelerations as well as previously mentioned calculated force rate, it is believed that these could have occurred as a result of the vertebral body fracture around the time of peak compressive force (approximately 70 ms) on the subject. These spikes had the largest effect on the reported peak resultant values in acceleration at S1 and L3, which made a significant contribution to the experimentally observed range and calculated standard deviation. Using the latest time derived from the force rate data (70.7 ms), peak resultant acceleration values were calculated and compared to determine the effects on the subject average and standard deviation. Minimal effect was found at higher instrumentation levels (T12) but significantly better agreement was seen at L3 and S1 by omitting post-fracture acceleration data. At L3, no difference was found in reported peak acceleration using this cut-off time compared to the entire dataset for PMHS2 and PMHS3. For S1 data, again no difference was found in the reported peak for PMHS2, and minimal difference was found for PMHS3 (Δ = 2 G). These peak values up to 70.7 ms for T12, L3, and S1 are shown in Table VI.

TABLE VI
PEAK SPINE LINEAR KINEMATICS SUMMARY FOR T12-S1 (TIME CUT-OFF 70.7 MS)

	Instrumentation	PMHS1	PMHS2	PMHS3	Average	Std Dev
T12	Peak resultant acceleration (G)	29.3	24.3	20.7	24.8	4.2
L3	Peak resultant acceleration (G)	29.8	27.1	27.3	28.1	1.5
S1	Peak resultant acceleration (G)	28.0	21.9	20.7	23.5	3.9

PMHS Lumbar Spine Force Estimates

Pressure data collected through the lumbar spine were used to estimate force transmission in the subjects. PMHS1 showed good agreement in calculated force between vertebral levels (avg = 6.2 kN, stdev = 0.3 kN), with no clear trend in changes up or down the lumbar spine. PMHS2 showed slightly less agreement between levels (avg = 8.5 kN, stdev = 1.5 kN) and trended opposite to what might seem intuitive, with calculated forces increasing at higher vertebral disc levels. Only two levels were successfully collected for PMHS3, but these showed an increase in calculated force at L5-S1 (8.2 kN) compared to L2-L3 (6.7 kN), which was expected.

Relative y-axis angular velocity of L3 with respect to S1 was calculated (Fig. 9a) to better understand local spinal kinematics at the levels where pressure measurements were recorded. These values were then used to determine relative flexion/extension for each of the three subjects (Fig. 9b). Angular displacement values showed consistent relative flexion of the lumbar spine during the event. Trends in angular displacement data were similar to that seen in the L5-S1 reported peak force values, with the highest calculated flexion seen in PMHS3 and the lowest in PMHS1. The contribution of flexion/extension combined with axial compressive loading on recorded intervertebral pressure is not fully understood. However, this could help explain the differences observed between PMHS as well as the increased calculated force at higher levels observed in some of the response data.

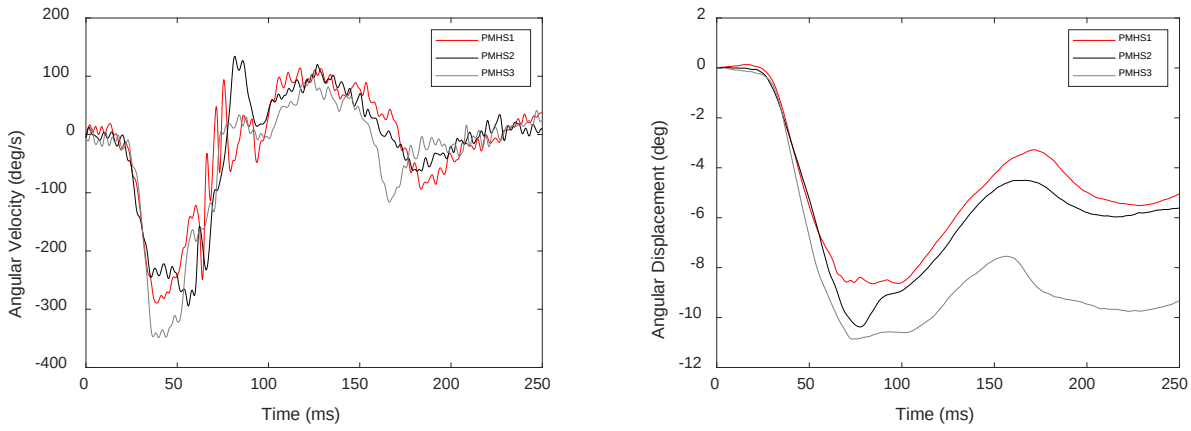

(a) (b)

Fig. 9. (a) Relative y-axis angular velocity of L3 with respect to S1 and (b) calculated angular displacement.

V. LIMITATIONS

The initial limitation of the outlined study is the current small sample size (N=3). This, combined with multiple data channel losses during testing, emphasizes the need for additional data to be generated before the data can be fully utilized for injury criteria development or FE-HBM validation. Additionally, because of the unique nature of the design of the harness, pre-tensions within the straps were not able to be captured, which may be important when implementing within a computational modeling environment and ensuring repeatability between test facilities.

Pre-test CT images were used to estimate the dimensions required for cross-sectional area calculations and subsequent force reporting. The process of doing this required manual interpretation of disc boundaries. Therefore, this process could have induced some error in the calculated values. Additional work was performed to determine the effect of manual disc area measurements taken using CT compared to the assumption currently made of a perfect ellipse for area calculation and measurements of anterior-posterior distance and left-right distance. Between the two methods an average percent difference of 4.5% was found within the area determined using the different methods. With respect to the reported force values, this difference in area had little effect on the PMHS peak average and standard deviation (initial area calculation method: avg peak force = 7.2 kN, stdev = 1.3 kN, CT area measurement method: avg peak force = 7.2 kN, stdev = 1.4 kN) however did slightly shift the overall range observed during testing (initial area calculation method: 5.8 kN to 9.8 kN, CT area measurement method: 5.9 kN to 10.3 kN). Additional work is being performed to refine this process for future data analysis using Mimics to create three-dimensional geometries of the individual intervertebral discs for determination of an average cross sectional area, which may prove more repeatable and minimize the variability currently observed in reported area measurements. An example of the geometry generation using mimics is shown in Fig. A7. The data that were collected for force calculations showed reasonable results when compared to the seat reaction force loads for the subject; however, more data are needed before it can be fully evaluated and utilized. Additionally, only a single pressure sensor inserted into the intervertebral disc center was used for the force estimation calculations. Because of this, the contribution of flexion or extension bending moment to pressure change is unknown. Additional instrumentation could be included in future studies to determine pressure gradients across the intervertebral disc to better describe local kinematics and overall contribution to reported pressure changes.

VI. CONCLUSION

PMHS vertical drop tower tests were successfully completed for three subjects. The instrumentation methodology evaluated during this round of testing showed positive results for the characterization of force transmission through the lumbar spine as well as vertebral body kinematics recorded in the lumbar and thoracic spine. Calculated lumbar spine force showed reasonable agreement between PMHS and recorded seat reaction force data. 6DX block data from S1 and L3 showed relative flexion in all PMHS subjects of the lumbar spine. The magnitude of flexion trended similar to the magnitude of calculated L5-S1 PMHS force values, suggesting a potential increase in intervertebral disc pressure with flexion, which has also been shown in previous studies [15]. Linear acceleration data between subjects were consistent up to the time of peak recorded seat force. Shortly after, PMHS1 S1 and L3 6DX blocks recorded large spikes in acceleration not observed in other PMHS testing. Spikes in calculated force rate data support the conclusion that these were likely caused as a result of PMHS1 experiencing a compression fracture at T10 during testing. Additional PMHS tests are planned for the same conditions, which should provide sufficient data for the development of PMHS response corridors for use in future FE-HBM validation work.

VII. ACKNOWLEDGEMENTS

First, we would like to sincerely thank the anatomical donors who make this work possible. We would like to thank all of the faculty, staff, and students of the Injury Biomechanics Research Center for their support with this and future work. We would also like to thank the individuals from the Air Force Research Labs who assisted with this test execution.

VIII. REFERENCES

[1] Mackenzie, C. (2019) “What it’s like to eject out of a military jet”. Internet: https://www.popsci.com/what-aircraft-ejection-is-like/. August 2019 [February 2023].
[2] Collins, R., McCarthy, G. W., Kaleps, I., Knox, F. S. (1997) Review of major injuries and fatalities in USAF ejections, 1981-1995. Biomedical Sciences Instrumentation, **33**: pp. 350–353. PMID: 9731384.
[3] Manen, O., Clément, J., Bisconte, S., Perrier, E. (2014) Spine injuries related to high-performance aircraft ejections: a 9-year retrospective study. *Aviation, Space and Environmental Medicine*.
[4] Epstein, D., Markovitz, E., Nakdimon, I., Guinzburg, A., Gordon, B. (2020) Injuries associated with the use of ejection seats: a systematic review, meta-analysis and the experience of the Israeli Air Force, 1990 – 2019. *Injury*, **51**: pp. 1489-1496.
[5] Sommer, F., Gadjradj, P., Pippig, T. (2023) Spinal injuries after ejection seat evacuation in fighter aircraft of the German Armed Forces between 1975 and 2021. *J Neurosurg Spine*, **38**: pp. 271-278.
[6] Mattock, M., Asch, B., Hosek, J., Boito, M. (2019) *The Relative Cost-Effectiveness of Retaining Versus Accessing Air Force Pilots.* Rand Corporation.
[7] Department of Defense (2014) Handbook, Airworthiness Certification Criteria (MIL-HDBK-516C).
[8] Destafano, L. (1972) National Technical Information Service, *Dynamic Response Index Minimization for Personnel Escape Systems.* Defense Technical Information Center.
[9] Toyota Motor Corporation (2021) Documentation, Total Human Model for Safety, AM50 Occupant Model Version 6.1.
[10] Elemance LLC (2021) Global Human Body Models Consortium User Manual: M50 Detailed Occupant Version 6.0 for LS-DYNA®.
[11] Hostetler, Z. S., Caffrey, J., Aira, J., Gayzik, F. S. (2022) Lower Extremity Validation of a Human Body Model for High Rate Axial Loading in the Underbody Blast Environment. *Stapp Car Crash Journal*, **66**: pp. 99–142. doi: 10.4271/2022-22-0004. PMID: 37733823.
[12] Aman, V., Anoop, C., Sudipto, M. (2023) Numerical investigation of THUMS (Total human model for safety) lower extremity FE model for under-body blast loading. *Materials Today: Proceedings*, **87**(Part 1): pp. 61–66, ISSN 2214-7853.
[13] SAE International Surface Vehicle Recommended Practice, “Instrumentation for Impact Test – Part 1 – Electronic Instrumentation”. SAE Standard J211-1, Rev. March 2014.
[14] Slykhouse, L., Zaseck, *et al*. (2019) Anatomically-based skeletal coordinate systems for use with impact biomechanics data intended for anthropomorphic test device development. *Journal of Biomechanics*, **92**: pp. 162–168.
[15] Demetropoulos C, Jangra J, Felon L, Garbec D. (2007) Intradiscal pressure mapping during in vitro tests – development of minimally invasive technique.

IX. APPENDIX A

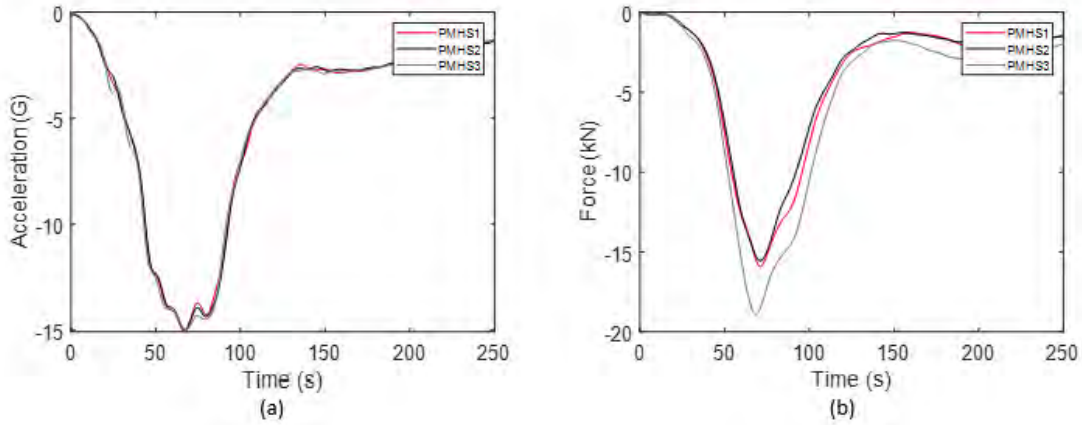

Fig. A1. Carriage time-history for (a) linear z-acceleration and (b) sum of seat pan reaction forces.

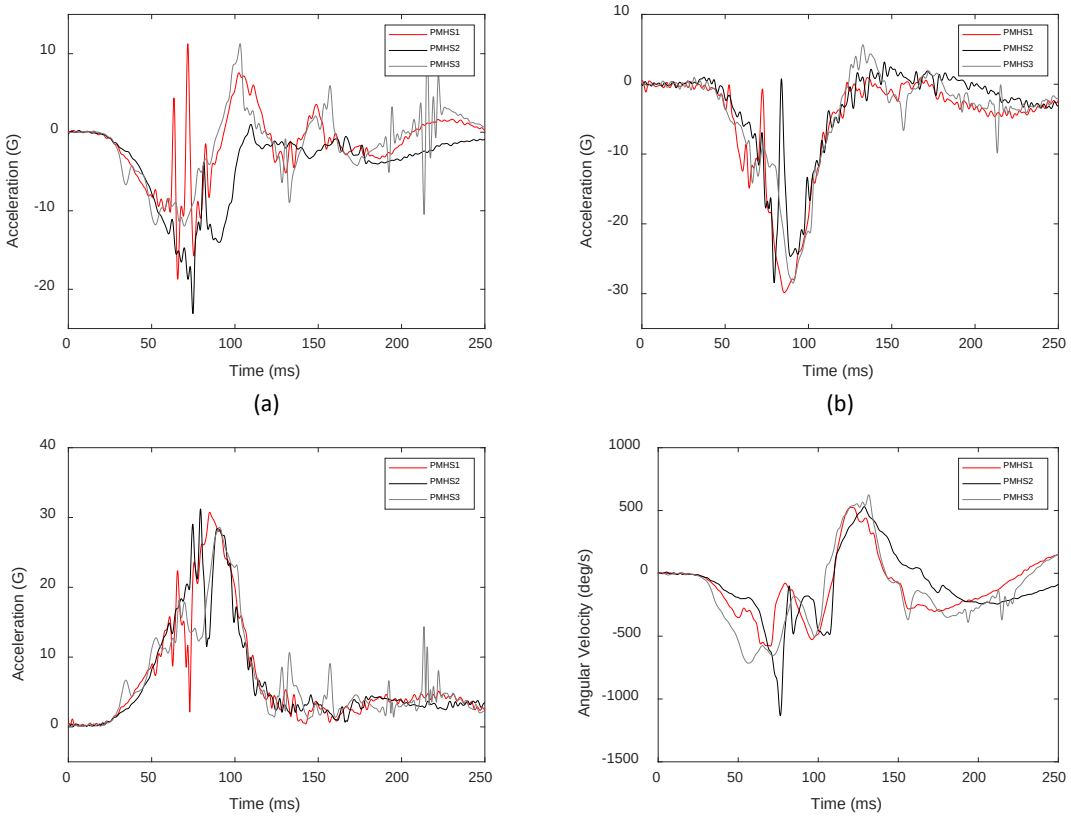

Fig. A2. T1 6DX time-history for (a) linear z-acceleration, (b) linear x-acceleration, (c) resultant linear acceleration, and (d) y-axis angular velocity.

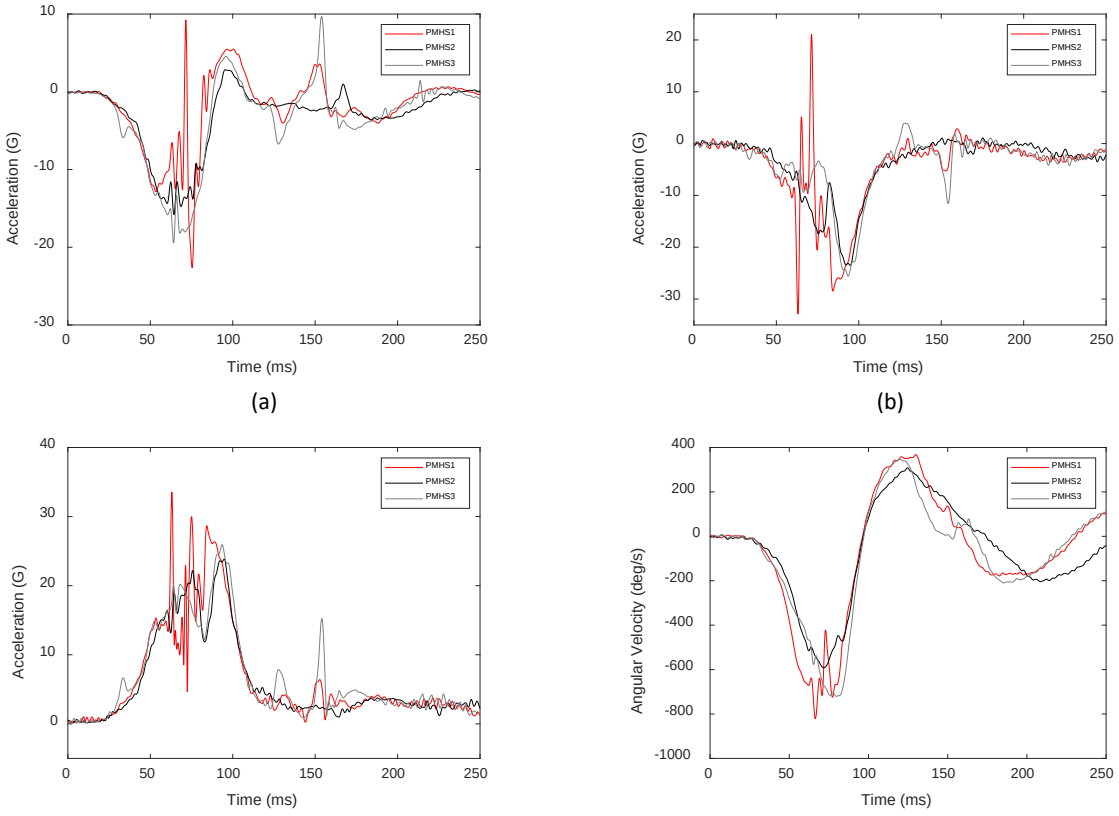

Fig. A3. T4 6DX time-history for (a) linear z-acceleration, (b) linear x-acceleration, (c) resultant linear acceleration, and (d) y-axis angular velocity.

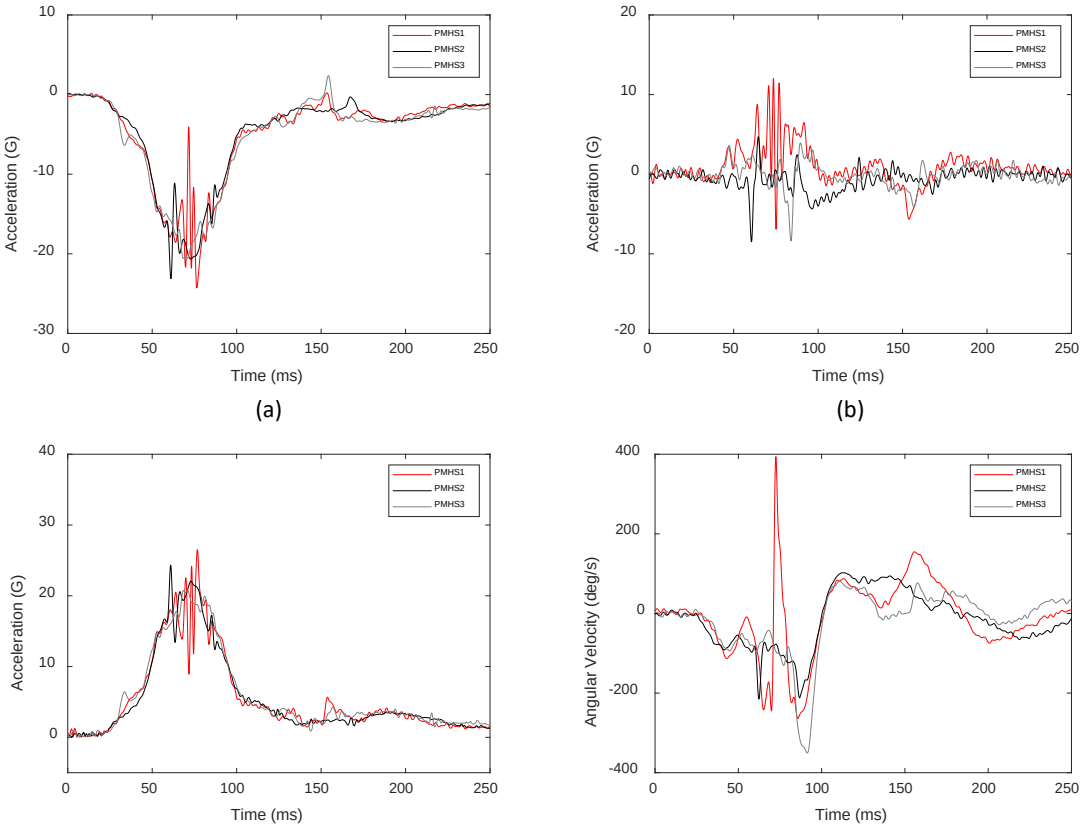

Fig. A4. T12 6DX time-history for (a) linear z-acceleration, (b) linear x-acceleration, (c) resultant linear acceleration, and (d) y-axis angular velocity.

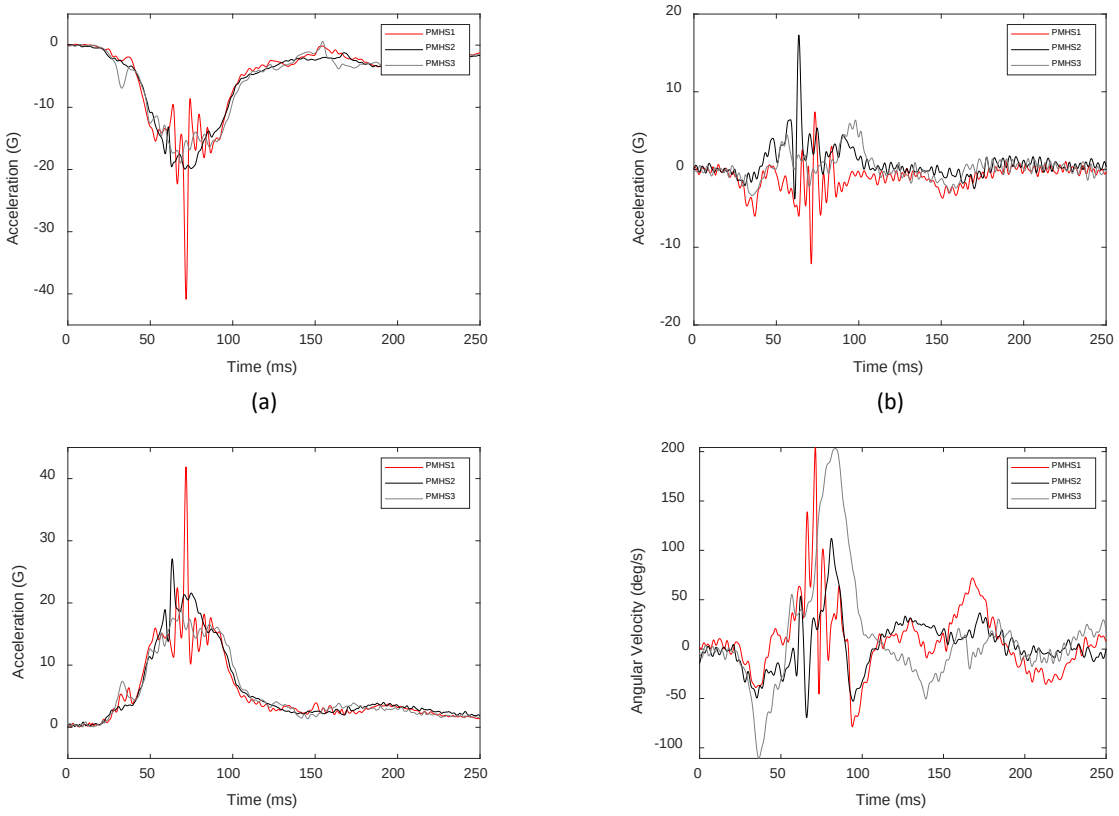

Fig. A5. L3 6DX time-history for (a) linear z-acceleration, (b) linear x-acceleration, (c) resultant linear acceleration, and (d) y-axis angular velocity.

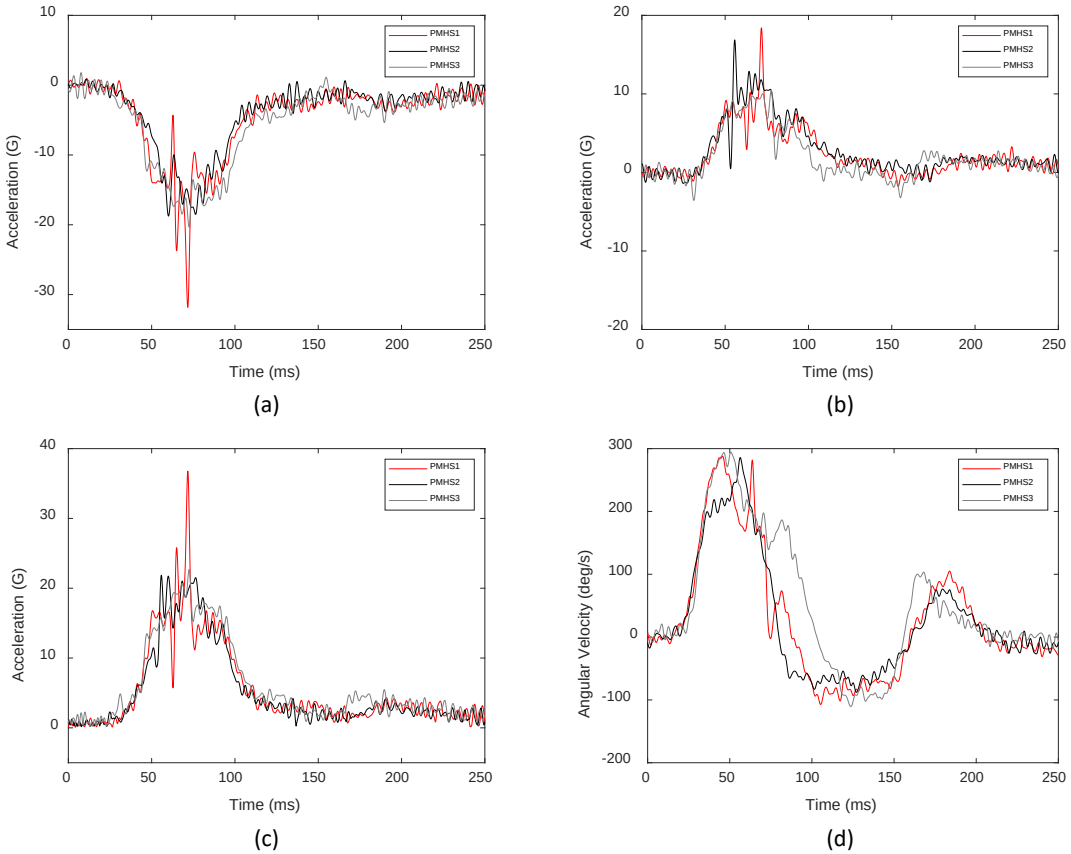

Fig. A6. S1 6DX time-history for (a) linear z-acceleration, (b) linear x-acceleration, (c) resultant linear acceleration, and (d) y-axis angular velocity.

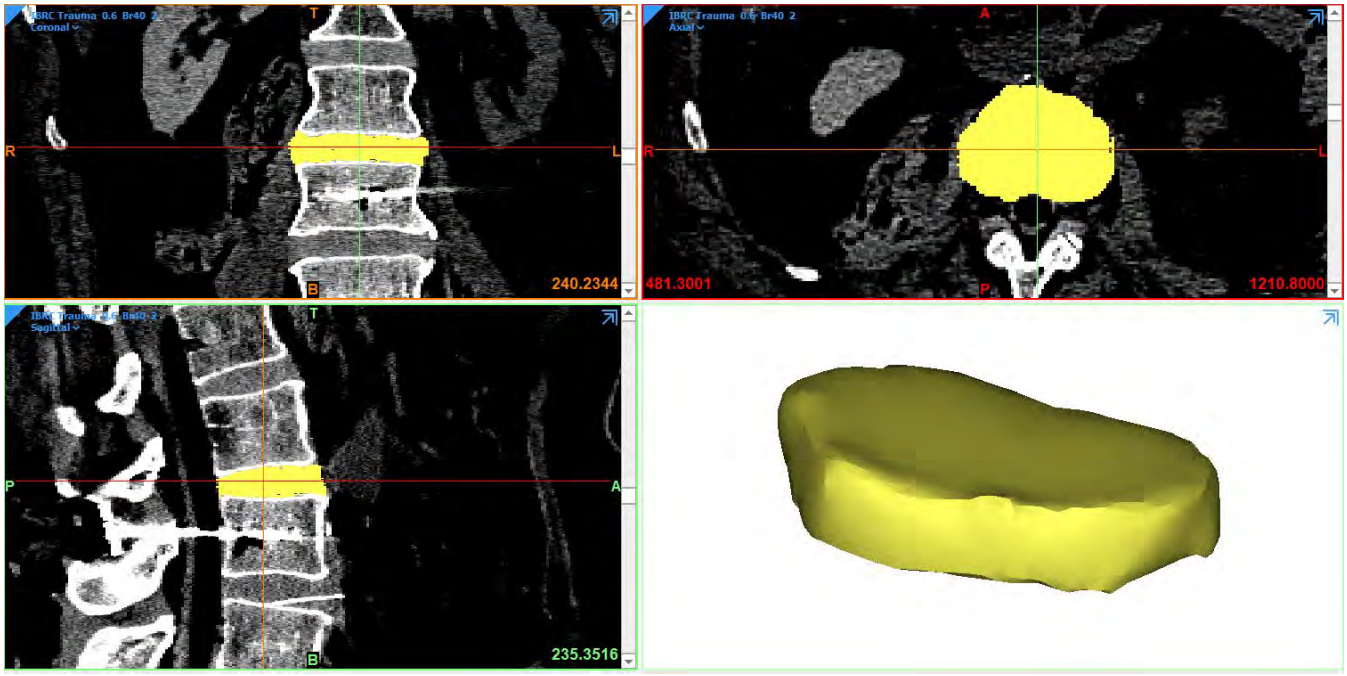

Fig. A7. Three-dimensional intervertebral disc model development using Mimics.